XIV. NEUROLOGY*

Dr. L. Stark
Dr. H. T. Hermann
Dr. Y. Okabe
Dr. G. Vossius
Dr. G. Zames

A. W. England
C. A. Finnila
L. A. Hoffman
W. Kipiniak
H. Levy
R. C. Payne

J. Redhead
H. Rhodes
A. A. Sandberg
P. A. Willis
L. R. Young

A. PATTERN RECOGNITION: for Electroencephalographic Diagnosis

For some time (1) we have considered the problem of automatic analysis of the electroencephalogram (a multiple display of simultaneous voltage functions derived from different areas of the head). The spectrum of one of these functions can be decomposed into several fairly narrow (±2 cps) bands of noise. These are interlaced with empirically

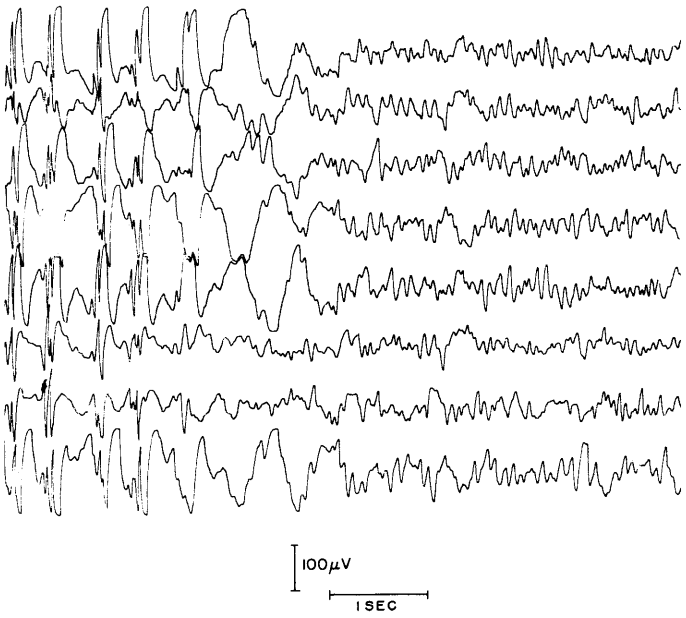

Fig. XIV-1. Multispike and wave burst recorded from 10-year-old epileptic child. The record after the burst is relatively normal.

recognizable higher-voltage wave patterns. Frequency analysis, including autocorrelation studies, has been insufficient to characterize these patterns, which are important features of the clinically useful description. An example of a spike-wave discharge in an epileptic child is shown in Fig. XIV-1.

*This research is supported in part by the U.S. Public Health Service (B-3055, B-3090); the Office of Naval Research (Nonr-609(39)); the Air Force (AF33(616)-7282); and the Army Chemical Corps (DA-18-108-405-Cml-942).

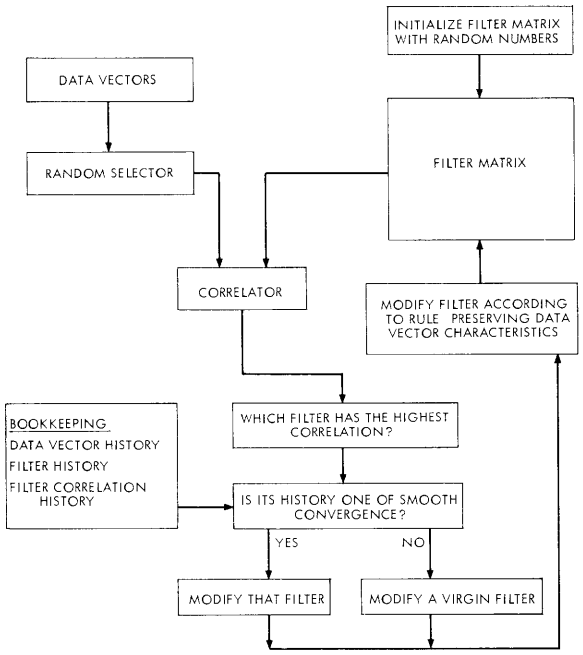

Fig. XIV-2. Flow diagram of the digital computer program for pattern classification. The filter matrix consists of n filters (row vectors) with m coefficients (m successive time function values). The data vectors also have m coefficients (m successive time function values).

One of the most attractive techniques in pattern recognition is based on matched filters. These have been utilized in bank-check reading systems (2). We considered the use of an analog adaptive matched filter similar to the one independently described by Jakowatz and others (3), but because of our desire to study multiple patterns (4), the experiments described below were performed on a digital computer.

The aim of the experiments was to determine the efficacy of simple rules in separating and classifying patterns that were independent in time (and thus presumably correlate with independent processes in the natural system under study). Orthogonality of the filters was not a goal.

Certain problems were circumvented initially. Artificial data were simulated. Also, rather than search for a correlation peak in time in order to time-match the data to the filter, data vectors (30 values of the time function) were used to construct a segmented time function. However, there was no training period during which the experimenter adjusted coefficients or structures in the classification scheme. The process of the pattern classification system can be understood by reference to Fig. XIV-2 and Fig. XIV-3. The program is initialized by inserting random numbers into the filter matrix and then introducing the set of data vectors. A single data vector is selected randomly and correlated with the set of recognition filters. The filter with the highest correlation is

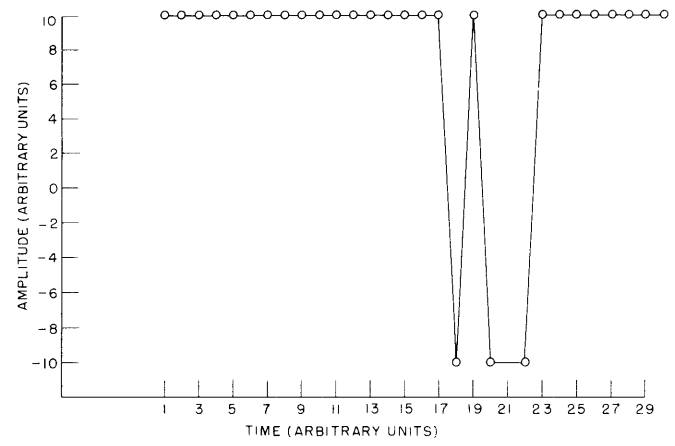

(a)

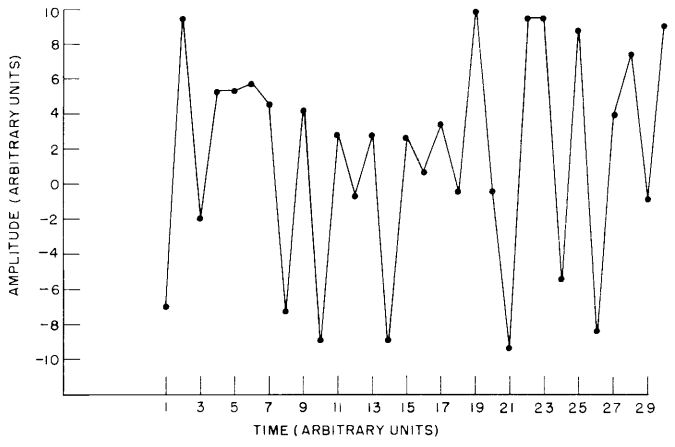

(b)

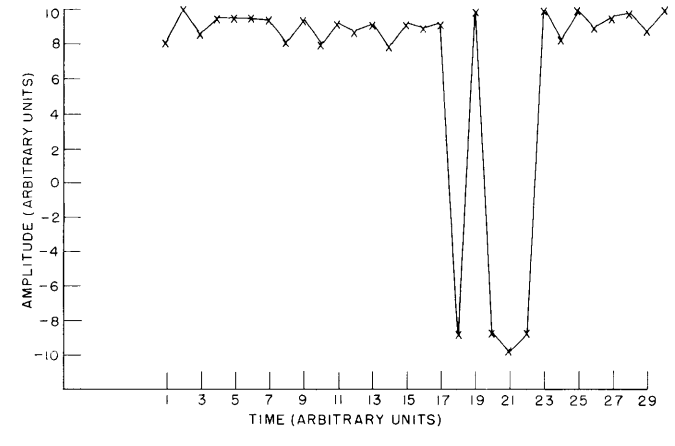

(c)

Fig. XIV-3. (a) Data vector no. 5 with m = 30 coefficients chosen to resemble a spike and wave. (b) Initialized filter no. 3 with m = 30 coefficients selected by a random-number generator. (c) Filter no. 3 after eight passes with data vector in (a). Note the marked fidelity of wave shape. The minor resemblance of (b) to (a) probably led to its selection at the first appearance of the data vector.

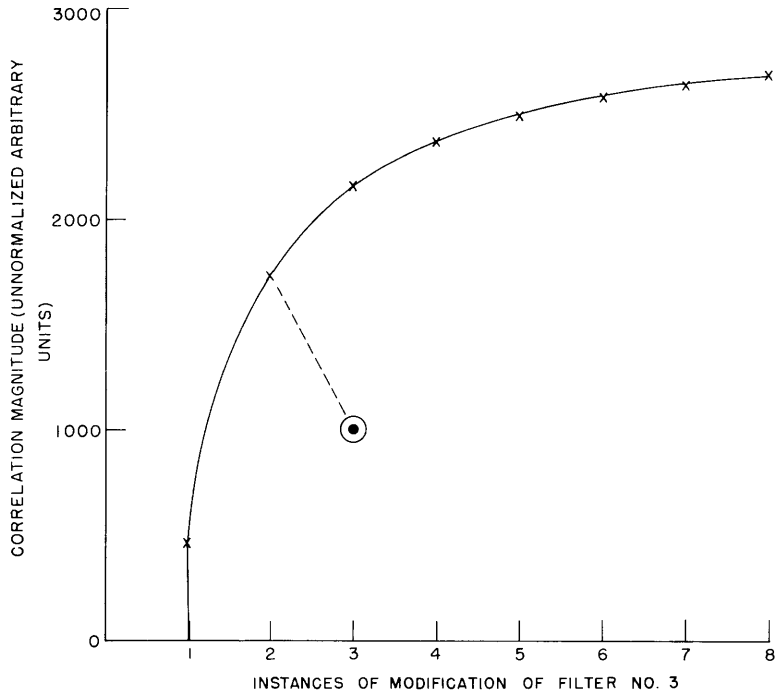

Fig. XIV-4. Smooth increase in correlation between filter no. 3 and the data vector no. 5 illustrated in Fig. XIV-3. This is a sign of the smooth convergence of the filter to the form of the wave pattern of the data vector. The large circled point is an imagined example of a correlation value that would have excluded its data vector from filter no. 3.

chosen for preliminary consideration. Its convergence history as displayed in Fig. XIV-4 is examined. This is possible because a record is kept of the correlation of each filter with the data vector on each instance of its final selection. For example, in Fig. XIV-4, filter no. 3 had correlations of 466 (unnormalized arbitrary units) on its first use and 1728 on its second use. If a data vector maximally correlated with filter no. 3 at the next presentation with a correlation of 1000, this would produce a greater-than-tolerable interruption of the filter convergence. Rather than permit this to occur, a virgin filter would therefore be used for that data vector and the bookkeeping adjusted accordingly. In scattered runs we have found correlations less than 0.95 of the previous value misleading.

The modification process consists merely of substituting a weighted sum of the filter coefficients and the data vector coefficients for the previous filter coefficients. This weighting gradually increases in favor of the previous filter coefficients. In this way a formed filter is resistant to environmental (data) perturbations.

The end product of a run is a set of formed filters resembling the wave patterns in the input time function, with auxiliary information such as the percentage of the time function represented by each filter.

Additional experiments in normalization techniques, pseudocorrelation, synchronization or time matching, finer discrimination, and utilization of real data are underway.

L. Stark

References

1. L. Stark, Memorandum on EEG Analysis, Section of Neurology, Yale University, New Haven, Conn., May 19, 1959. I am grateful for discussions with Dr. P. Friedlander, P. A. Willis, and M. Goodall.

2. For an excellent review of the whole field, see M. Minsky, Steps toward artificial intelligence, Proc. IRE 49, No. 1, p. 8 (Jan. 1961).
See, also, A. L. Samuel, Some studies in machine learning using the game of checkers, IBM J. Res. Develop. 3, 211-219 (July 1959).

3. C. V. Jakowatz, R. L. Shuey, and G. M. White, Adaptive waveform recognition, Report No. 60-RL-2435E, General Electric Research Laboratory, Schenectady, N. Y., May 1960.

4. I am grateful to Dr. W. Helvey, Republic Aviation Corporation, for making his IBM 7090 computer available to me and to Mr. N. Levine for help with programming and debugging.

B. USE OF ON-LINE DIGITAL COMPUTER FOR MEASUREMENT OF A NEUROLOGICAL CONTROL SYSTEM

In a previous report (1) an account was given of the dynamic characteristics of the motor coordination system. In that report the requirement for a complex unpredictable

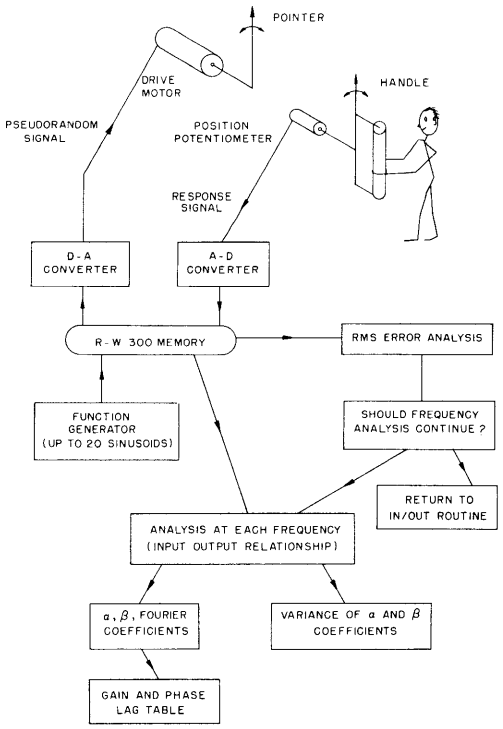

Fig. XIV-5. Flow diagram of experimental apparatus, computer arrangement, and analysis program.

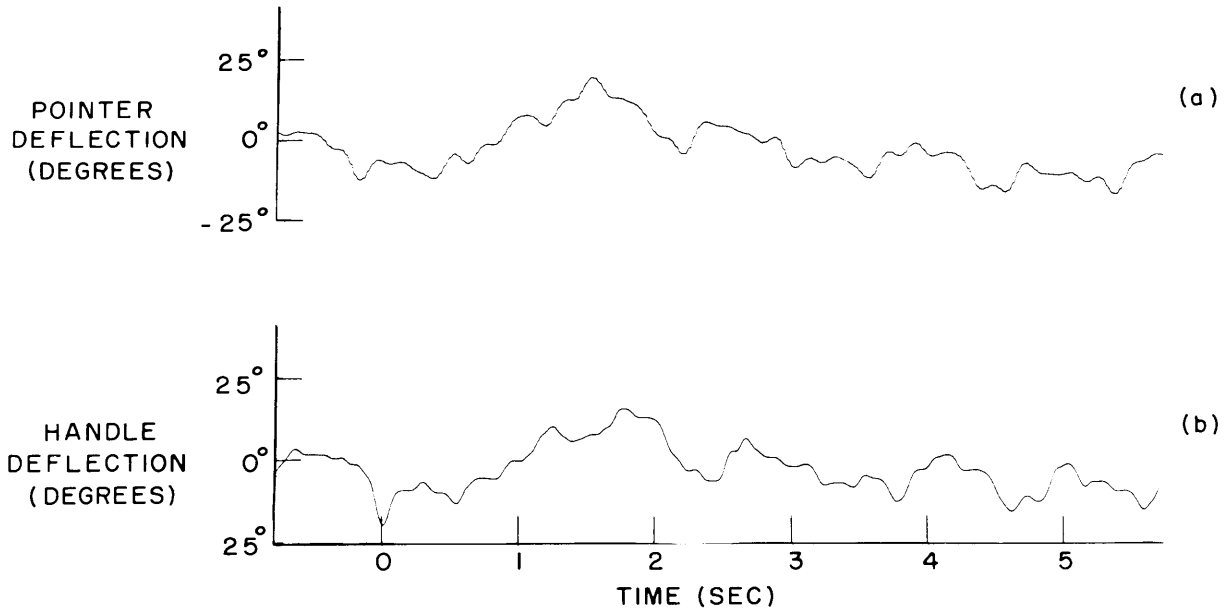

Fig. XIV-6. The computer-generated function (a) is fed into the pointer drive motor of the motor coordination testing apparatus. The handle deflection (b) is the subject's response. This figure shows a portion of the 25-sec total run. Note the subject's phase lag, which is apparent in responses to the higher frequency components.

Table XIV-1. Output data from electric typewriter of the computer.

RMS 3.

FREQ:	COSVAR	SINVAR	PHASE	GAIN
0.0996	217.	41.	40.	3.046
0.1247	284.	490.	351.	-5.570
0.1599	167.	651.	8.	-0.468
0.1999	165.	470.	11.	-0.468
0.2500	176.	698.	24.	3.671
0.3117	404.	292.	346.	0.468
0.3942	346.	511.	3.	-1.679
0.4992	371.	278.	351.	0.000
0.6237	373.	425.	356.	0.000
0.7888	372.	454.	7.	0.000
0.8818	404.	354.	354.	0.000
0.9987	294.	332.	359.	0.000
1.2507	189.	449.	7.	0.000
1.6647	238.	324.	0.	-0.906
1.8750	180.	238.	6.	-1.015
2.1447	202.	386.	17.	-1.156
2.5017	146.	245.	24.	-1.335
3.7500	82.	174.	15.	-1.585
5.0097	93.	148.	80.	-4.429
7.5000	51.	96.	34.	-6.015

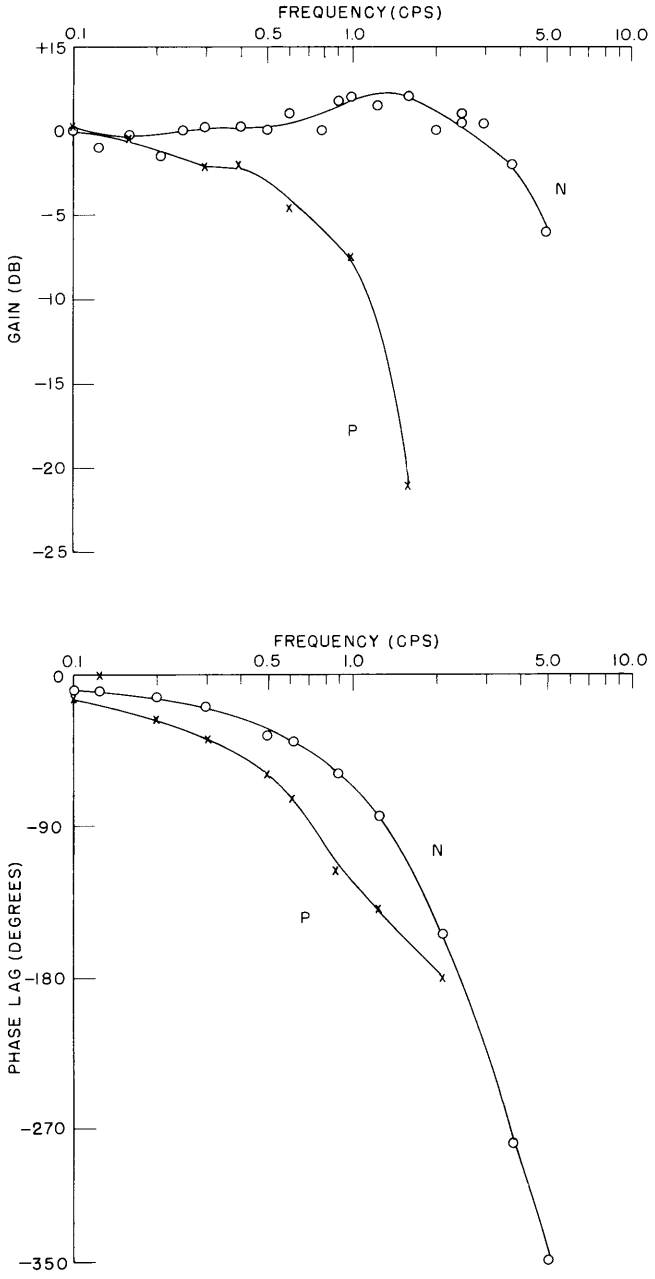

Fig. XIV-7. Bode plot, showing response of normal subject, N, and of a patient with Parkinson's syndrome, P. The normal subject's data are the result of 6 runs, and each point is an average of 3 values. Note the evident difference between the normal and abnormal responses. Root-mean-square errors for N were either 22 or 23, and for P were between 24 and 27. Perfect following would result in an rms of zero; no following at all would result in an rms of 63.

input is made clear. In order to meet this need, reduce the hidden errors in analyzing filtered data, permit shorter experiments (and thus less dependence upon assumptions of time invariance), and eliminate painstaking pencil-and-ruler analysis we have inaugurated an on-line digital computer system for this and related experiments. The RW-300 computer is a magnetic-drum (8000 18-bit words), solid-state computer that is often used in process control applications. It has integral analog-to-digital and digital-to-analog conversion facilities.

The program (2) is outlined in the flow diagram of Fig. XIV-5. The function generator produces a sum of as many as 20 sinusoids, specified as to frequency and amplitude, which is then converted to an analog voltage and fed to a mechanical input to the subject. His mechanical response measured as an electrical voltage is reduced to digital form and stored in the computer in real time. The computer-generated and subject response functions are shown in Fig. XIV-6.

In the analysis routine the total rms error for 26 seconds of tracking is measured. If this seems to indicate a reasonable experimental result, the analysis program then proceeds to determine the α and β Fourier coefficients cycle by cycle, frequency by frequency. For each frequency the mean α and β coefficients are used to determine gain and phase lag at that frequency. The variance of the α and β coefficients for each frequency is also determined (3). Table XIV-1 shows a portion of such an analysis.

The Bode plot in Fig. XIV-7 shows the response of a normal subject compared and contrasted with the response of a patient with Parkinson's syndrome (4). It is evident that the data points are consistent and that our method is sensitive to quantitative differences in the organization and function of the neurological control system for hand movement.

The real-time experiment takes only 26 sec. The cleanup analysis for a 10-frequency pseudostochastic signal is completed in 14 minutes (2 minutes for rms error analysis, 2 minutes for normalization, and 1 minute per frequency). Formerly, 2 hours for running and 2 days for analysis were required.

Y. Okabe, R. C. Payne, H. Rhodes, L. Stark, P. A. Willis

References

1. L. Stark, M. Iida, and P. A. Willis, Dynamic characteristics of motor coordination, Quarterly Progress Report No. 60, Research Laboratory of Electronics, M.I.T., Jan. 15, 1961, pp. 231-233.

2. Our thanks to Dr. P. Friedlander, D. Fellows, and E. Brooks, of the Thompson-Ramo-Wooldridge Products Company, Beverly Hills, Calif., for programming and debugging help.

3. P. Schultheus and F. Kuhl, Project Report, Department of Electrical Engineering, Yale University, 1959. This study demonstrated the non-Gaussian distribution of phase lag of a signal in band-limited noise.

4. Dr. R. Schwab, Neurology Department, Massachusetts General Hospital, Boston, is cooperating with us in studying neurological patients.

C. ASYMMETRICAL BEHAVIOR IN THE PUPIL SYSTEM

In performing transient experiments on the pupil a surprising asymmetrical response was observed. Evidence will be adduced concerning the responsible natural system characteristics.

The method of exciting and measuring the pupil system has recently been reviewed (1). The measurement depends upon differential reflectivity of iris and pupil to infrared light. Each subject has a particular reflectivity index that is obtained by calibrating before each experiment. Photocell voltage as a function of pupil area determined from a series of flash photographs is displayed in Fig. XIV-8.

Positive pulses of light producing pupillary contractions and subsequent redilatations are shown in Fig. XIV-9. These indicate a weighting function related to the transfer function

$$G(s) = \frac{0.16\, e^{-0.23s}}{(1+0.1s)^3}$$

as obtained from steady-state experiments (1).

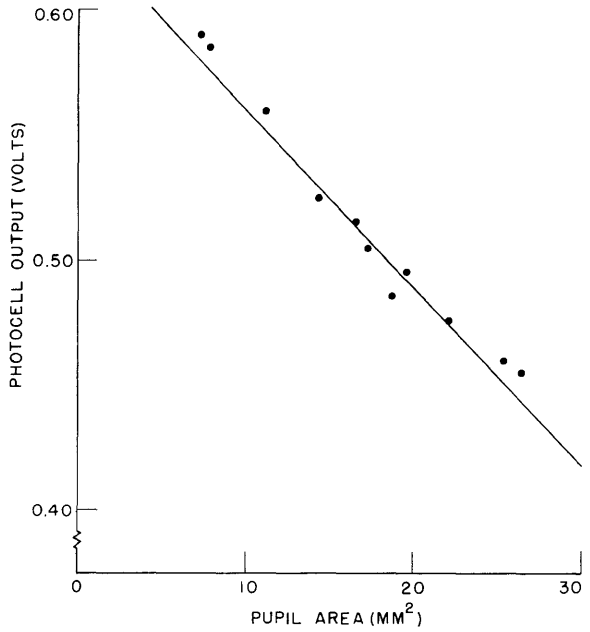

Fig. XIV-8. Calibration graph: voltage output of the pupil-area photocell (infrared) as a function of pupil area measured from flash photographs using a magnifying (7X) graticule with 0.1 mm divisions.

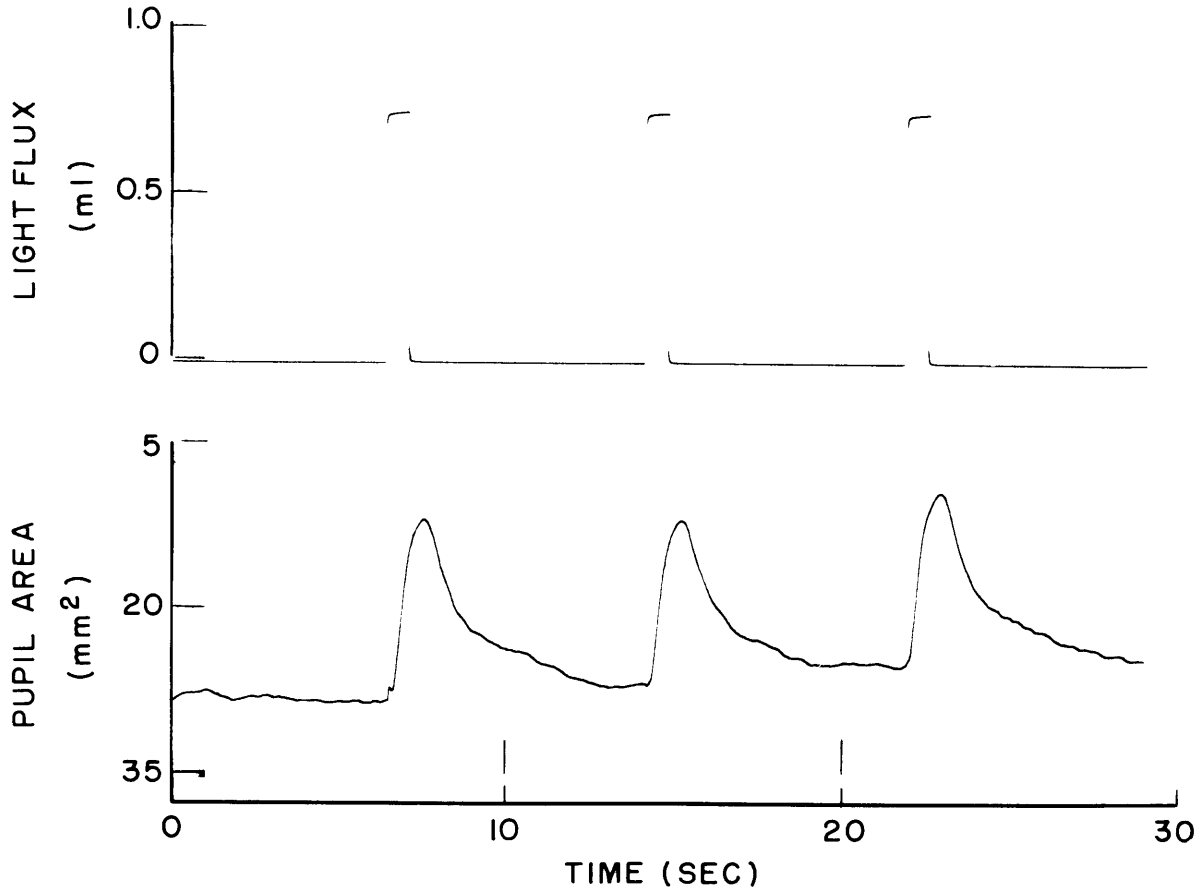

Fig. XIV-9. Positive pulses of light which produce pupillary contractions. Note that the base line is fairly regular because of the low biological noise level in the dark.

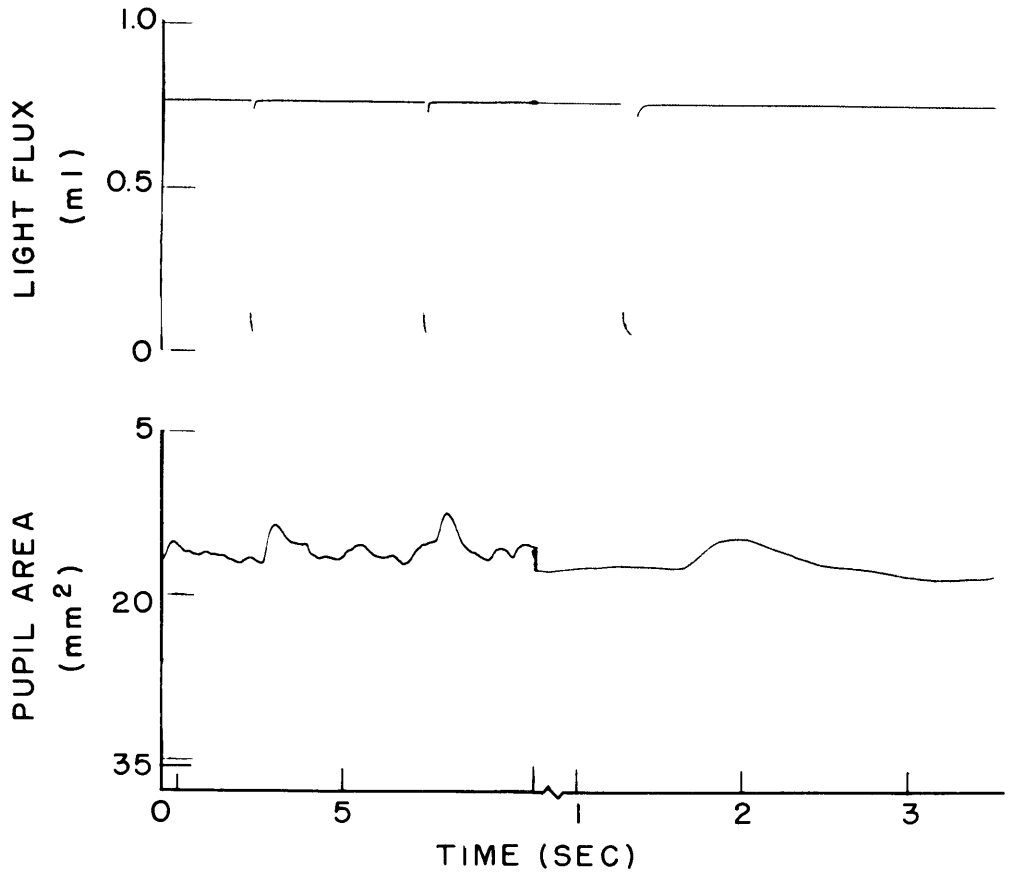

Fig. XIV-10. Sharp negative pulses of darkness from a set light level also produce pupillary contractions. Note the irregular base line because of the high biological noise level, which occurs when the retina is exposed to a bright light. There is a change of time scale during the recording so that the response can be seen in detail.

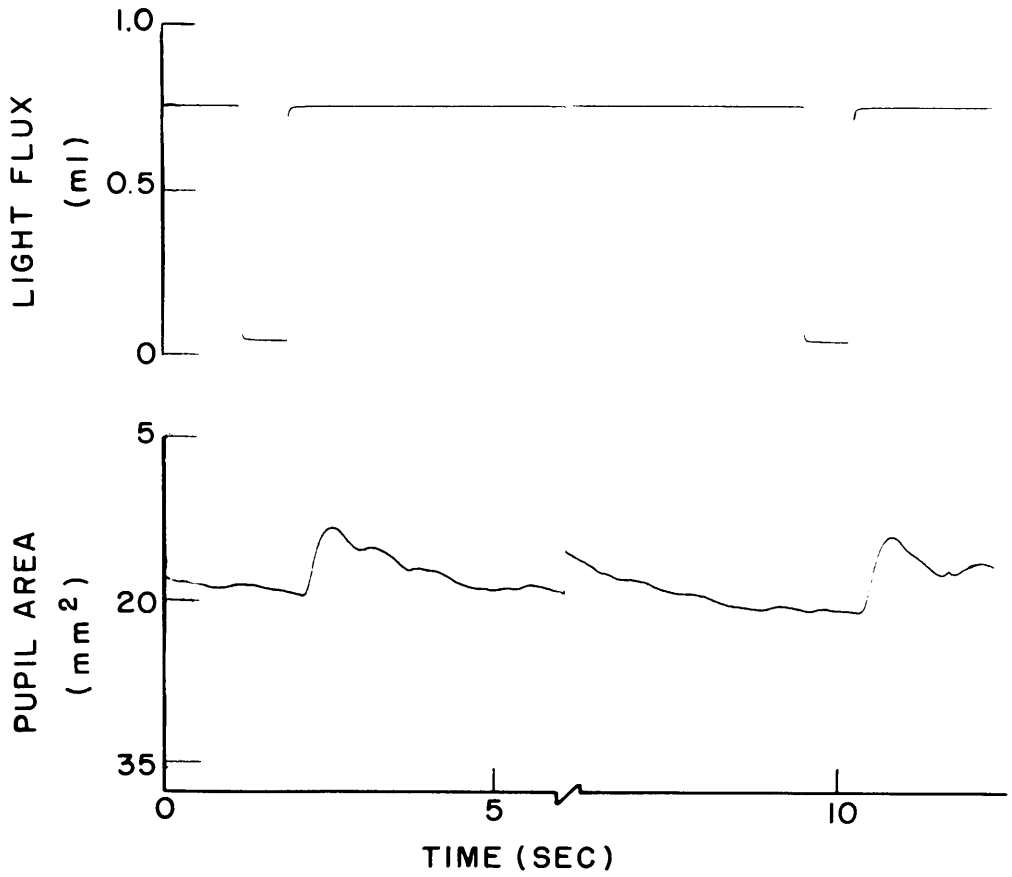

Fig. XIV-11. Negative pulses of longer duration clearly show that the contraction occurs about 0.23 sec after the end of the negative pulse. Thus the pupil system is really responding to the return of the light level.

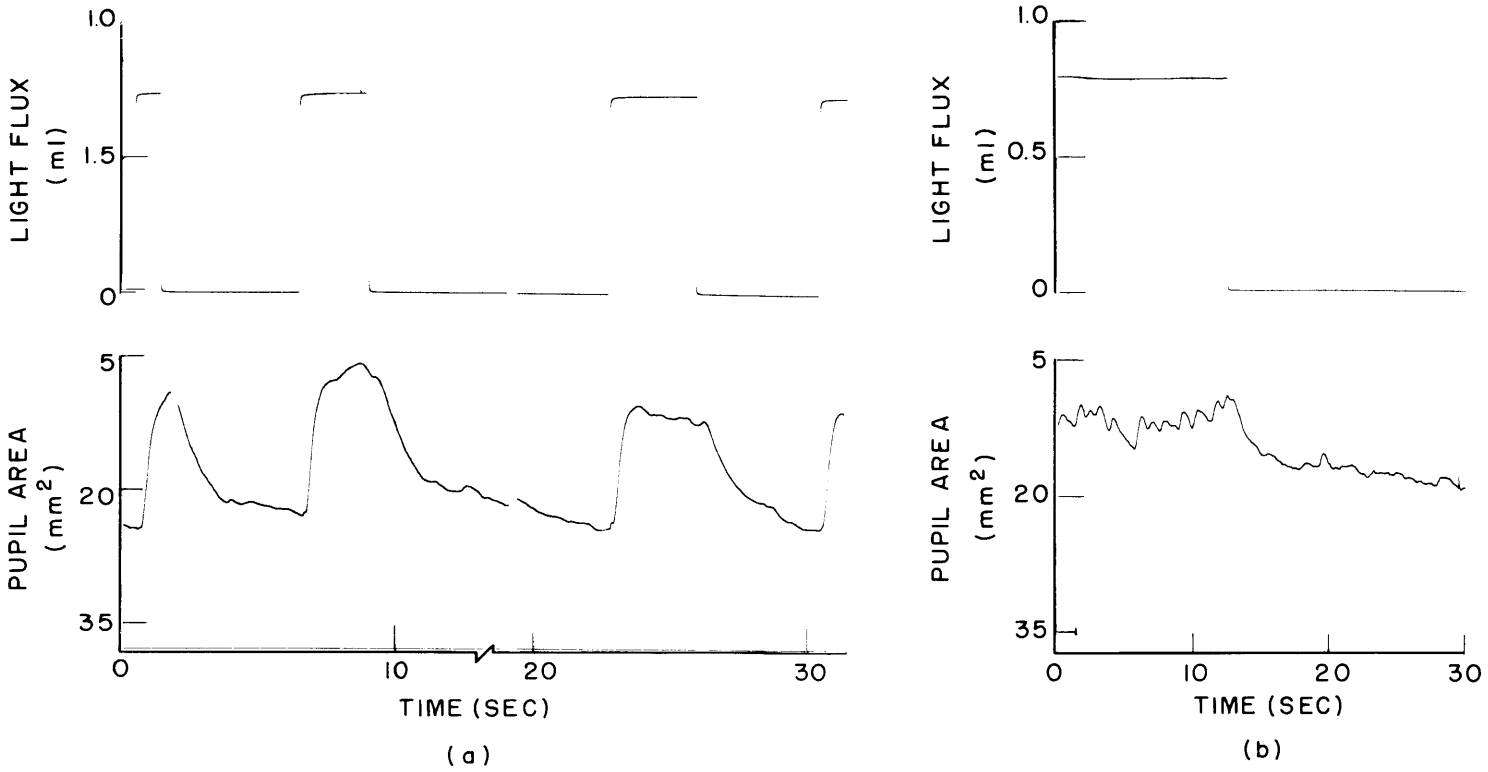

Fig. XIV-12. Transient responses from which appropriate time constants for pupillary contraction and dilatation can be obtained. Note the asymmetry.

Surprisingly, when negative pulses (pulses of relative darkness) are used, the pupil system responds with a contraction and subsequent redilatation as shown in Fig. XIV-10. Either the pupil system is behaving in an unusual manner for a regulating system or a special case is being observed.

When the width of the negative pulse is increased, it becomes evident that the pupil is not responding to the negative side of the pulse but to the return to the original light level. The experiment illustrated in Fig. XIV-11 clearly shows that the contraction occurs about 0.23 sec after the end of the negative pulse.

By referring to the positive pulse experiments in Fig. XIV-9 it can be seen that the pupil has a 0.23-sec transport delay, at the end of which the triple lag dynamics forms the shape of the response. This substantiates our demonstration that the pupil system does not respond to negative pulses per se.

Why is this so? There is an asymmetry in the time constants of pupillary contraction and dilatation. In addition to the transport delay, dilatation has a time constant of approximately 2 sec (a time-varying and nonlinear function). Therefore a considerable time period may elapse before dilatation occurs to any degree after a negative step. However, if one waits long enough, dilatation does effect a return

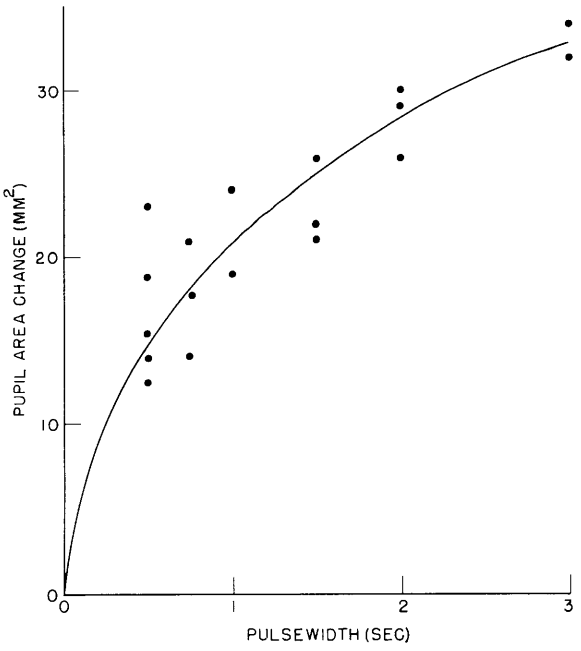

Fig. XIV-13. Increase in pupil response with increasing width of the negative pulse. This is a measure (nonlinear because of nonlinearities in the pupil response) of the increase in retinal sensitivity with time in the dark (dark adaptation). The time constant of dark adaptation under these experimental conditions is approximately 1.3 sec.

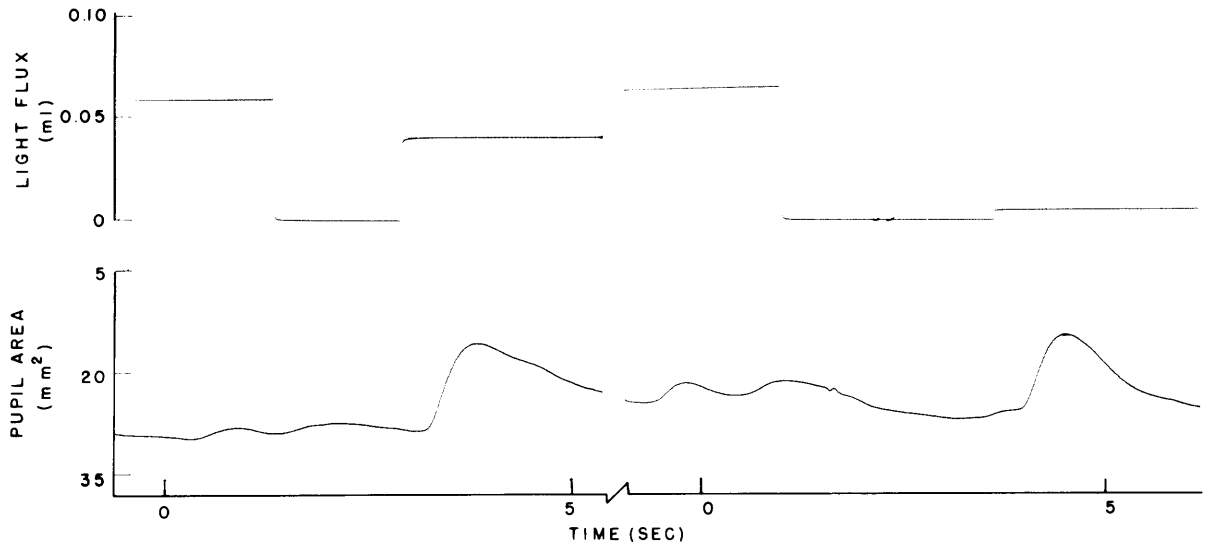

Fig. XIV-14. By changing the light flux level to which the negative pulse returns, the size of the pupillary response is varied. This enables us to utilize the null method of estimating retinal sensitivity.

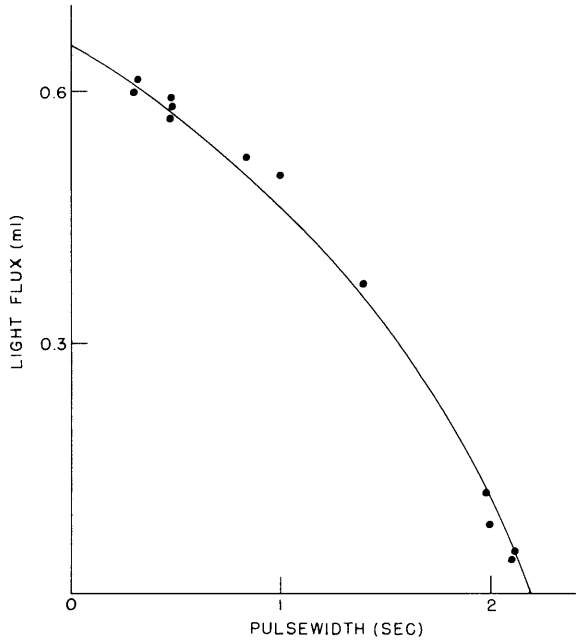

Fig. XIV-15. The amplitude of the return step which maintains a constant pupil response. This amplitude as a function of negative pulsewidth gives us an inverse measure of retinal sensitivity as a function of dark adaptation time.

of the pupil area to its operating level. Figure XIV-12 shows several examples of step changes of light at different time scales, which illustrate this point.

We now turn to the question of why a level of light to which the pupil-retinal system has adapted can act as a stimulus. It must be that during the brief period of the negative pulse, retinal sensitivity rapidly rises, so that the reapplication of the original light level is now an effective stimulus. An increase in retinal sensitivity to light caused by exposure to darkness is termed dark adaptation. Generally, time constants for dark-adaptation processes are approximately 120 seconds. The negative-impulse, dark-adaptation process seems to be very much faster, perhaps several orders of magnitude. Mostly, dark adaptation has been studied in psychosensory brightness-matching experiments, which are unable to define rapid dark adaptation.

In Fig. XIV-13 is shown a plot of pupil area change as a function of the width of the negative pulse. This is a rough guide to the dark-adaptation process, although we know that the pupil response is generally proportional to the log of the stimulus. However, we are led to an estimate of 1.3 sec for the time constant of this rapid dark adaptation.

By using the more refined technique shown in Fig. XIV-14 we may be able to obtain more precise measures of this process. Here we adjust the level of light to which the pulse returns.

Now, the size of the pupillary response can be controlled in two ways: by varying the width of the negative impulse and the amplitude of the return step. After selecting a particular size of pupil response we can find at each negative impulse width a return step amplitude that will produce the selected size response. In this way, we obtain a measure of retinal sensitivity as a function of time for dark adaptation. Such a plot is shown in Fig. XIV-15.

In summary, we have demonstrated the effect of asymmetries in the pupil-retinal system in producing a seemingly anomalous result: unidirectional responses to excitation by impulses of either sign. In the course of experiments elucidating this phenomenon we have discovered and measured a rapid retinal dark-adaptation process.

J. Redhead, L. Stark, R. C. Payne

References

1. L. Stark, Stability, oscillations, and noise in the Human Pupil Servomechanism, Proc. IRE 47, No. 11, p. 1925 (Nov. 1959).

D. RANDOM WALK RESPONSE OF THE CRAYFISH

The crayfish is a small aquatic invertebrate selected for study in our laboratory because the easy accessibility of its nervous system permits recording of nerve impulse signals by simple electrode probes (1).

The crayfish (see Fig. XIV-16) has a pair of cephalic ordinary eyes capable of spatial perception. In addition, it possesses a primitive photosensitive tail ganglion, which even in the absence of normal visual input, permits a light-avoidance behavior. This response induces the animal to seek out and remain in dark environments, provided that no overriding stimuli exist (2-5).

Fig. XIV-16. Crayfish: Note the cephalic eyes capable of orienting the claw thrusts with accuracy. The primitive photosensitive ganglion is located under the tail.

By stimulating the photosensitive ganglion with a controlled light source and fixing the leg to a strain gauge, regular sequences of this random walk response can be shown, as in Fig. XIV-17.

Our aim is to study, in this favorable preparation, the complex interaction of signals in nervous pathways. A first stage of our research is to record these nerve signals along the path of the random walk response. Figure XIV-18 shows our arrangement for monitoring the light input signal to the photosensitive ganglion, the nerve impulses along the ventral nerve cord to the thoracic ganglion, the nerve impulses in the motor nerve to the leg muscles, and the tension produced by the muscles.

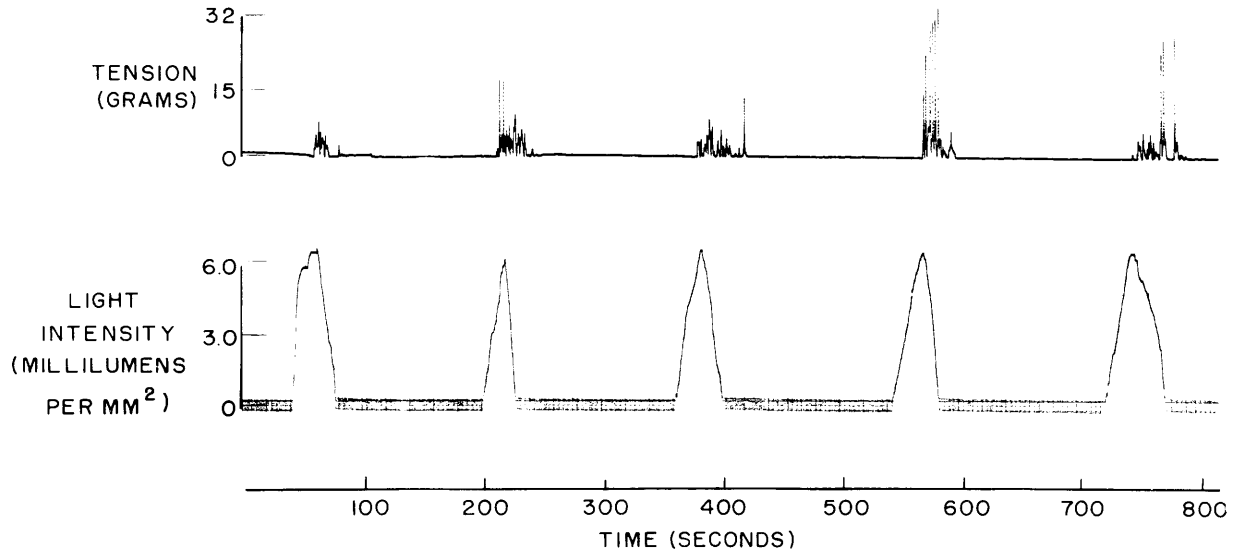

Fig. XIV-17. Random walk response. Note regularity of response. The experimenter turned the light off when the response occurred, thus preserving light sensitivity.

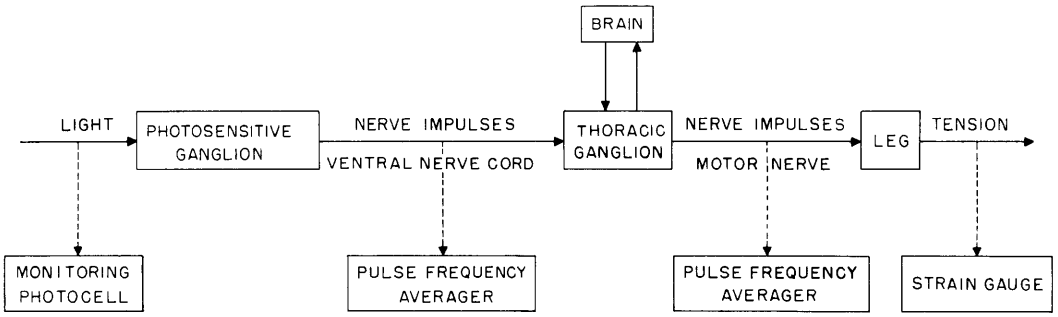

Fig. XIV-18. Experimental arrangement for monitoring input, output, and nerve impulses. The nerve impulses were amplified, selected by a pulse amplitude window, pulse-shaped, and averaged by an RC lagging element.

Simultaneous recordings of these quantities are shown in Fig. XIV-19. Here we see the successive appearance of the signals: light, ventral cord impulses, motor nerve impulses, and tension.

Note that the random walk response seems to last for relatively fixed periods of 80 ± 20 sec. Therefore, any simple dynamical relationship must be attempted with caution. Further evidence for the complexity of this response is the marked regularity obtained by blocking the complex cephalic eyes, and conversely, blocking of the response by strong light stimuli to these eyes.

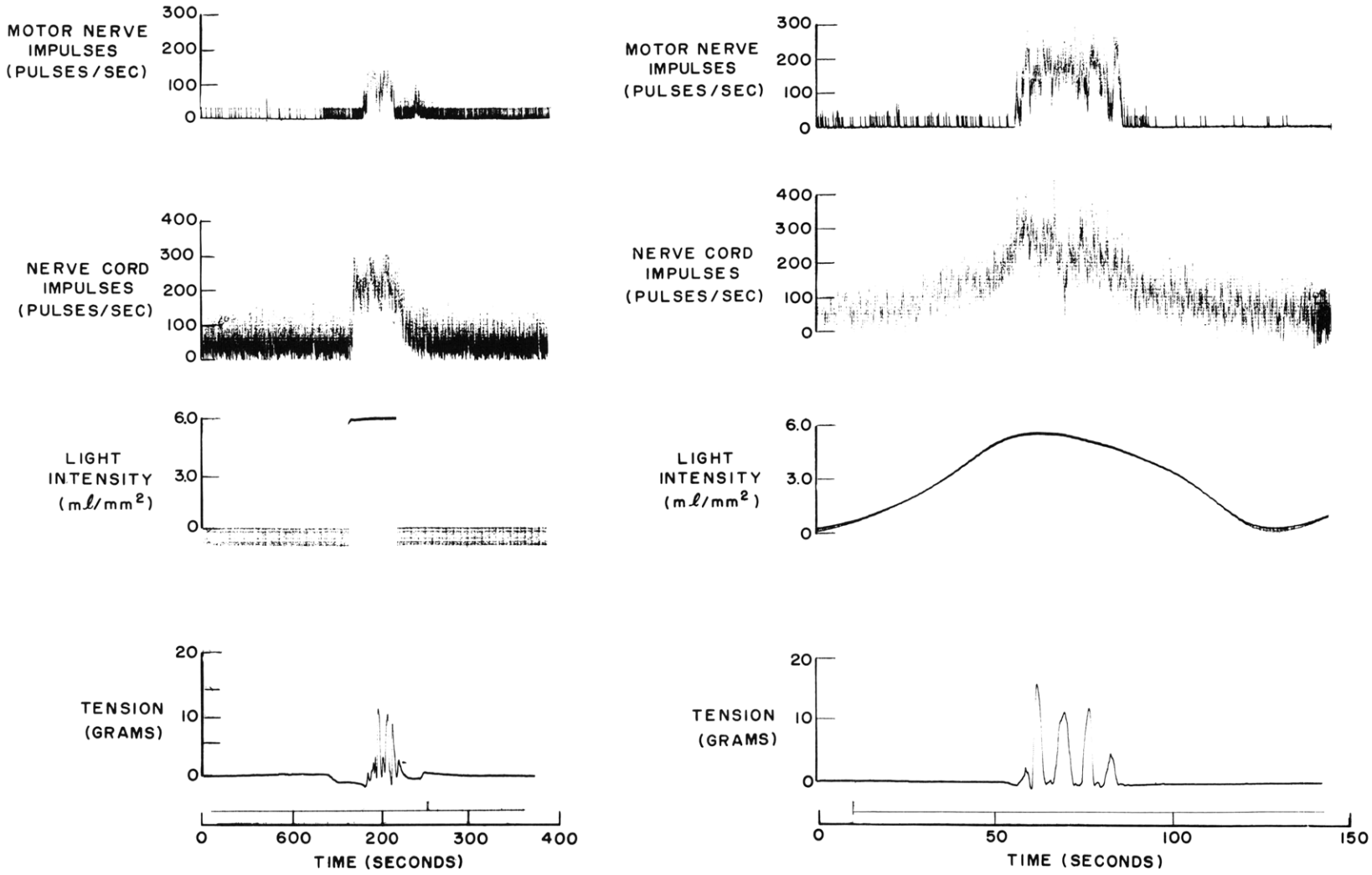

Fig. XIV-19. Random walk response. This experiment displays monitored light input, averaged frequency of ventral nerve cord nerve impulse, averaged frequency of motor nerve impulse, and leg tension. The illuminated area of the crayfish was maintained at 1 mm^2, the area just sufficient to cover the photosensitive ganglion.

The interweaving of low-priority background responses, such as the random walk response, with high-priority behavior, such as attention to strong visual stimuli, may provide a clue to the mechanisms that permit the crayfish, despite its small brain size and limited repertory of behavioral response, to meet the requirements of everyday living.

H. T. Hermann, L. Stark

References

1. L. Stark, Transfer Function of a Biological Photoreceptor, Technical Report 59-311, Wright Air Development Center, August 1959.

2. C. L. Prosser, Action potentials in the nervous system of the crayfish. II. Responses to illumination of the eye and caudal ganglion, J. Cell. and Comp. Physiol. 4, 363-377 (1934).

3. J. H. Welsh, The caudal photoreceptor and responses of the crayfish to light, J. Cell. and Comp. Physiol. 4, 379-388 (1934).

4. B. Kropp and E. V. Enzmann, Photic stimulation and leg movement in the crayfish, J. Gen. Physiol. 16, 905-910 (1933).

5. C. A. G. Wiersma, Giant nerve fiber system of the crayfish. A contribution to comparative physiology of synapses, J. Neurophysiol. 10, 23-38 (1947).

6. D. Kennedy, Responses from the crayfish caudal photoreceptor, Am. J. Ophthalmol. 11, 46(3), 19-26 (1958).

E. NEUROLOGICAL ORGANIZATION OF THE CONTROL SYSTEM FOR MOVEMENT

This report presents some simple experiments that indicate the effects of changes in the motor coordination control system. Surprisingly, these marked reorganizations occur with change in mental set.

Experimental conditions and background are presented in part in a previous report (1), which shows how the dynamics of the motor coordination system change according to input. Especially contrasted were predictable (simple sinusoids) and unpredictable (mixtures of three prime sinusoids) input wave functions. Figure XIV-5 shows the apparatus that constrained the movement to a wrist rotation and provided for the angular position of the handle to be recorded (2).

When the subject was instructed to rotate the handle back and forth as rapidly as possible, a record similar to the top line of Fig. XIV-20 was obtained. During the high-velocity portion of the movement the antagonists (opposing muscles) were quite relaxed and limp. Because of this inactivity, in spite of marked stretching of the antagonists by the agonists (contracting muscles), it is concluded that the stretch reflex was inoperative. Either the afferent feedback from the muscle spindle was markedly reduced or it was functionally ineffective in exciting the alpha motor neurons (final common path).

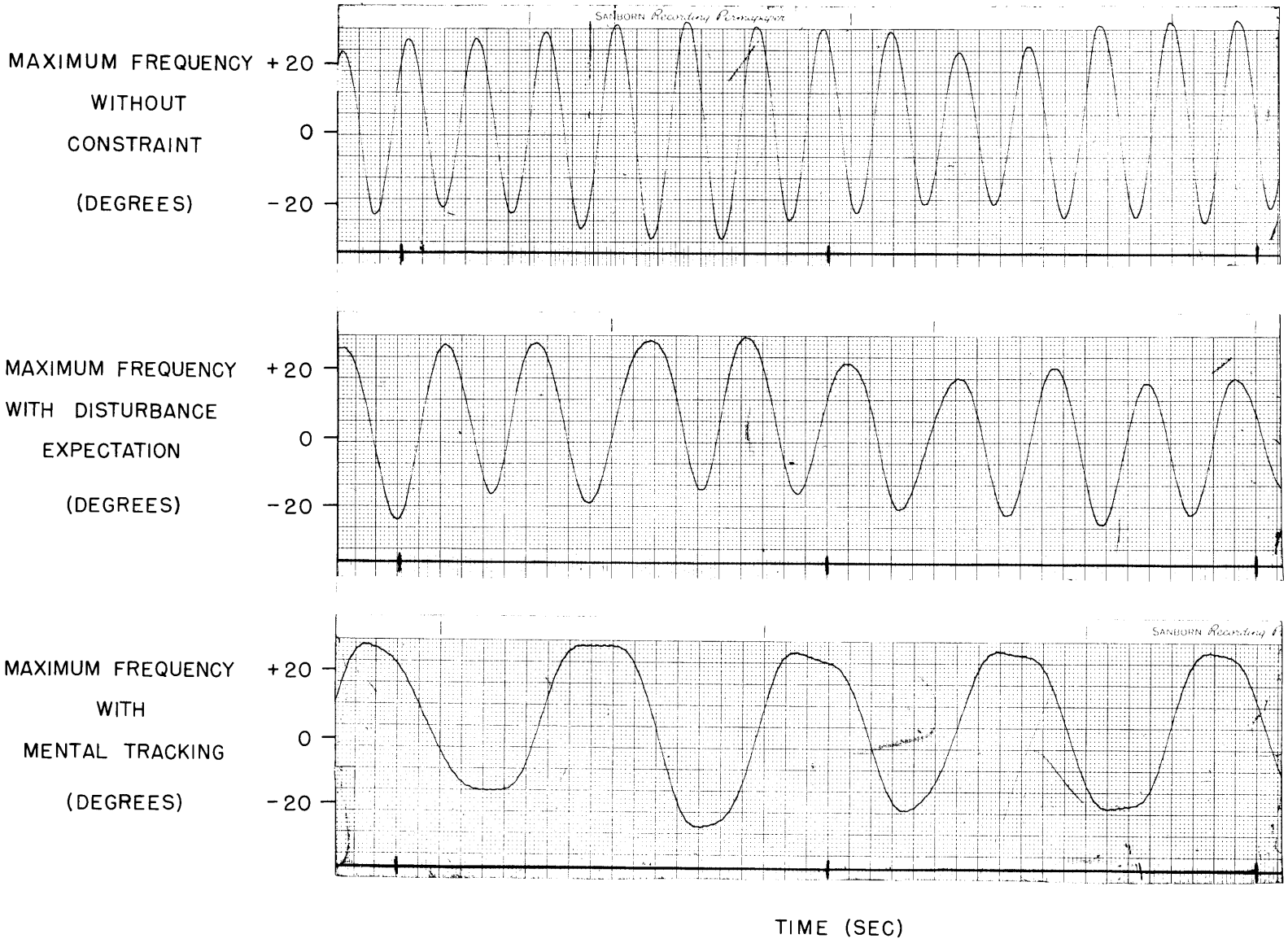

Fig. XIV-20. Freewheeling experiment.

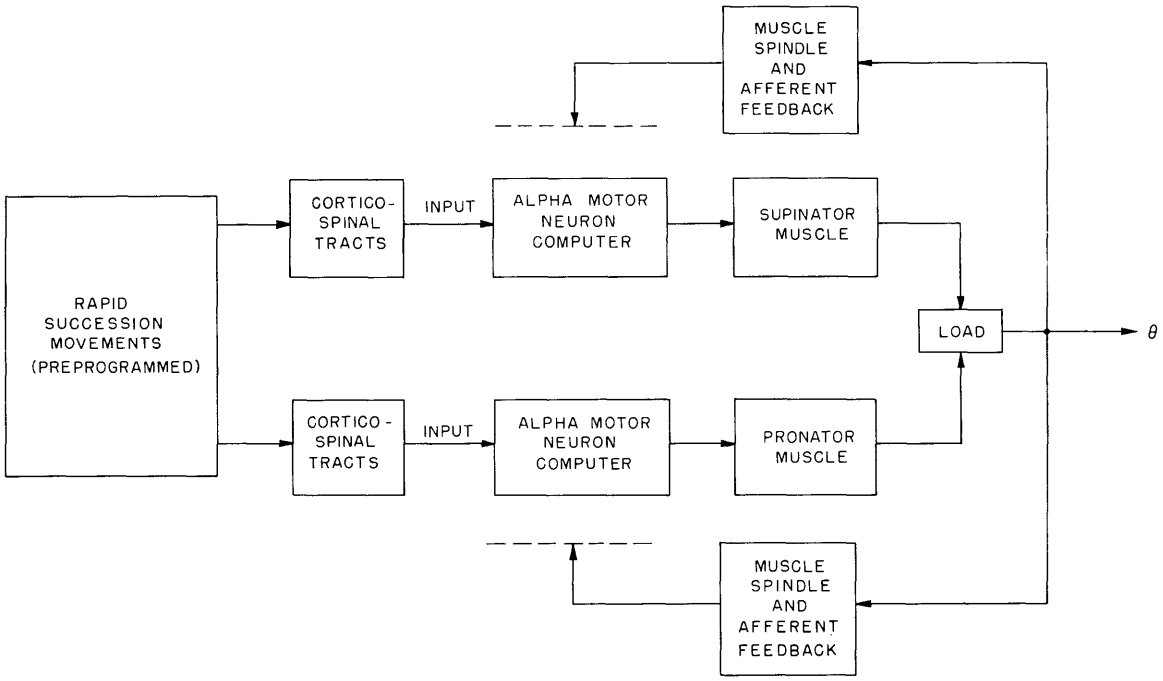

Fig. XIV-21. Rapid-succession movements: freewheeling.

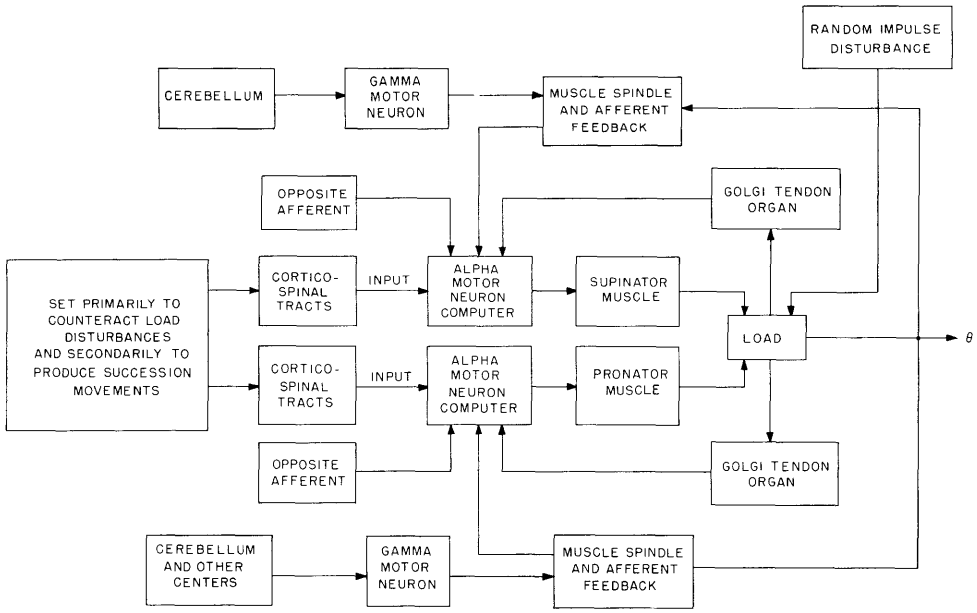

Fig. XIV-22. Position servocontrol set primarily to counteract load disturbances.

Figure XIV-21 shows a simplified block diagram of the situation. It is important to note: (a) the back-to-back pair of control systems (agonist-antagonist) that are always present in movement because of the inability of muscle to push, (b) the open-loop mode that permits the high-frequency oscillation, and (c) the preprogrammed set of alternating contractions sent down from the brain.

The subject was instructed to perform successive movements again, but this time he was told that his primary object was to prevent deflection of his hand by random input disturbances. Only secondarily was he to oscillate his hand at as high a frequency as possible. Figure XIV-22 shows the nature of the neurological organization in this mode of operation. The essential features here are: (a) the muscle spindle system, acting as a high-gain length regulator; (b) the resultant increased stiffness or spring constant of both agonists and antagonists; (c) the sharing of the alpha-motor neuron (final common path) by this length regulator and the cortico-spinal input. As a result of these factors the frequency of oscillations is slowed as shown in the middle recording of Fig. XIV-20.

This, incidentally, elucidates the essential nature of the rigidity of Parkinson's syndrome. Here the spindle length-regulator is always (except in sleep) on full gain and thus opposes the weakened cortico-spinal inputs. It might be well to mention that diffuse anatomical organization of the gamma input makes it a highly inappropriate followup servo system. In fact, it is not used for this function, but for postural tone and end-of-movement damping and clamping.

In the final set of instructions given the subject he was asked to imagine a pointer moving back and forth, to track this imaginary pointer, and then attempt to oscillate

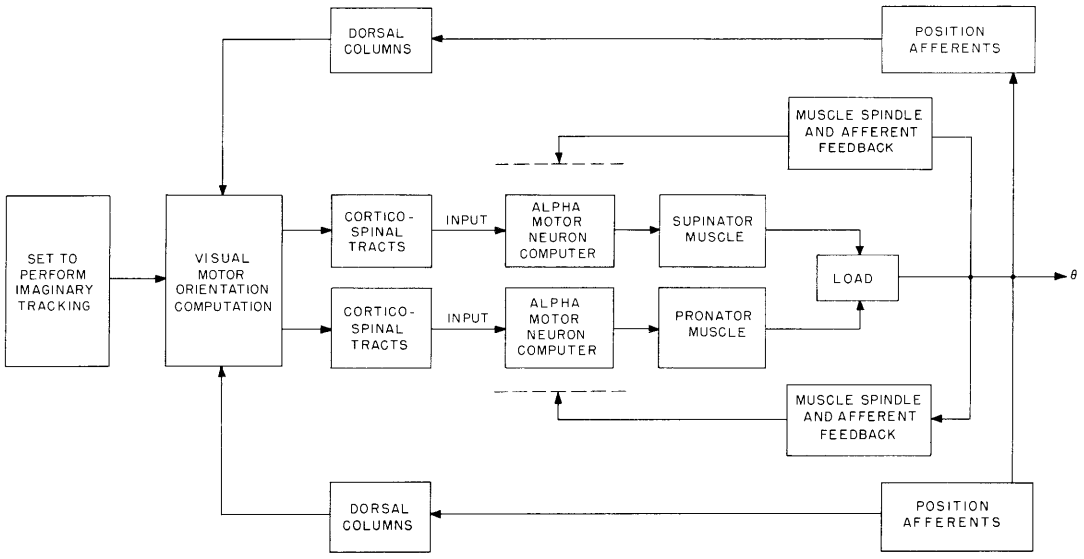

Fig. XIV-23. Mental tracking mode configuration.

his hand as fast as possible, as in the first mode. The arrangement of the neurological apparatus is shown in Fig. XIV-23. The position afferent information feeds back to a visual-motor orientation complex that is postulated to exist in the brain. Perhaps, because of the necessity to transmit and process all control signals through the imagery of the mental-tracking process, the oscillation is markedly slowed. This is shown in the bottom recording of Fig. XIV-20.

The gamma-spindle system may be utilized in this mode at the end of each high-velocity portion of the oscillation. Evidence for this comes from an experiment done with Dr. G. Rushworth (3). The gamma gain controls to the spindles were blocked with procaine, producing the so-called cerebellar syndrome of hypotonia, asthenia, ataxia, overshooting, rebound, dysmetria, and postural drift. Skilled voluntary movements were still possible with attention (4). However, when sinusoidal tracing was being performed, similar in principle to mental tracking, errors were made in a particular fashion. Occasionally, at the end of the high-velocity portion of the sinusoid the pencil hand would continue in the tangential direction without halt. This indicates that the damping and clamping functions of the length regulator (spindle) were being called for, and thus that they would be normally active in a like manner.

In summary, we have tried to define by experiment another facet of the complexity of the neurological control of movement – the ability to change the actual organization of the multiloop neural system (5).

L. Stark

References

1. L. Stark, M. Iida, and P. A. Willis, Dynamic characteristics of motor coordination, Quarterly Progress Report No. 60, Research Laboratory of Electronics, M.I.T., Jan. 15, 1961, pp. 231-233.

2. L. Stark, M. Iida, and P. A. Willis, Dynamic characteristics of the motor coordination system in man, Biophys. J. 1, 279-300 (1961).

3. L. Stark and G. Rushworth, Voluntary Movement without Gamma Efferent Innervation, Technical Report, Neurology Section, Yale University, May 1958.

4. R. S. Woodworth, The accuracy of voluntary movement, Psychol. Rev. 8, 350-359 (1899).

5. I wish to thank J. Atwood, Dr. J. Elkind, and P. A. Willis for valuable discussions and suggestions.